The Gradient System.

Understanding Gradients from an EM Perspective: (Gradient Linearity, Eddy Currents, Maxwell Terms & Peripheral Nerve Stimulation)

Franz Schmitt
Siemens Healthcare, Business Unit MR
Karl Schall Str. 6
91054 Erlangen, Germany
Email: Franz.Schmitt@Siemens.com

1 Introduction

Since the introduction of magnetic resonance imaging (MRI) as a commercially available diagnostic tool in 1984, dramatic improvements have been achieved in all features defining image quality, such as resolution, signal to noise ratio (SNR), and speed. Initially, spin echo (SE)[(1)] images containing 128x128 pixels were measured in several minutes. Nowadays, standard matrix sizes for musculo skeletal and neuro studies using SE based techniques is 512x512 with similar imaging times. Additionally, the introduction of echo planar imaging (EPI)[(2,3)] techniques had made it possible to acquire 128x128 images as produced with earlier MRI scanners in roughly 100 ms. This improvement in resolution and speed is only possible through improvements in gradient hardware of the recent MRI scanner generations. In 1984, typical values for the gradients were in the range of 1 - 2 mT/m at rise times of 1-2 ms. Over the last decade, amplitudes and rise times have changed in the order of magnitudes. Present gradient technology allows the application of gradient pulses up to 50 mT/m (for whole-body applications) with rise times down to 100 µs. Using dedicated gradient coils, such as head-insert gradient coils, even higher amplitudes and shorter rise times are feasible. In this presentation we demonstrate how modern high-performance gradient systems look like and how components of an MR system have to correlate with one another to guarantee maximum performance.

2 Gradients and its leading role in fast MRI

In MRI, the attainable resolution, δx, is inversely proportional to the gradient-time integral, $\int_{T_{RO}} G_R(t)dt$, over the readout period T_{RO} as shown in Figure 1. When the measurement time for a particular MR sequence (see Figure 2) is to be shortened without sacrificing resolution, the gradient amplitude, G_R, must increase and rise time, T_R, decrease. We will discuss later how this may be realized. In this section we only concentrate our efforts on the particular case of a gradient echo-sequence with flow compensation of Figure 2 and how the improved gradients affect the design of fast imaging schemes. Figure 2a) shows a conventional GRE RO gradient pulse waveform with flow compensation. Using faster gradients the flow compensating gradients can be shortened while the echo time, TE, may be kept unchanged (Figure 2b) despite the lower readout bandwidth used, improving the SNR of the measurement. The echo time can also be

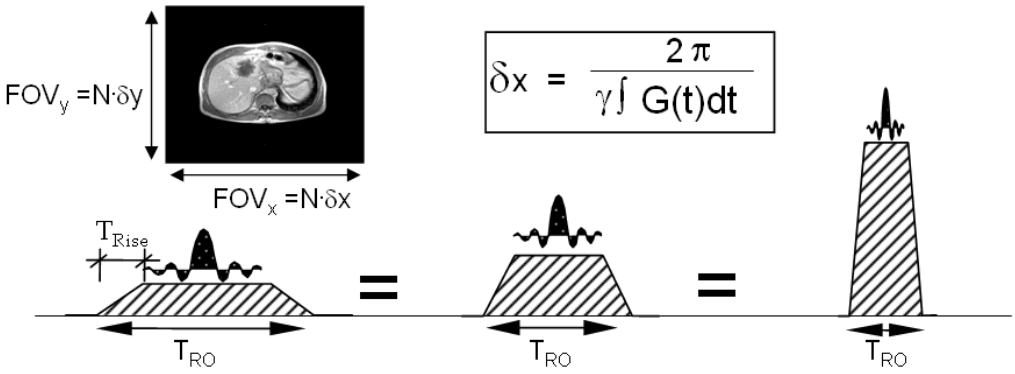

Figure 1: Upper row: Image resolution and its correlation to the gradient-time integral (shaded area). Lower row: Gradient amplitude G_R must increase and rise time T_R must decrease to keep the gradient area.

shortened (Figure 2c) to allow more data lines to be acquired at the same SNR, if the imaging time is kept the same as for the conventional sequence of Figure 2a. Finally, when the shortest TE possible is chosen (Figure 2d) faster scanning compared to the cases illustrated in Figures 2a-c is possible. Nonetheless, this will result in images with reduced SNR because of the higher readout bandwidth. Thus, depending on speed or resolution any of the above schemes may be chosen to acquire the data. Dynamic cardiac imaging (motion involved) will benefit from a sequence using the scheme of Figure 2d. For morphological imaging (no motion involved), such as for neuro imaging, sequences using readout as shown in Figures 2b or 2c may be used as they allow higher resolution with similar imaging times as with the conventional sequence of Figure 2a.

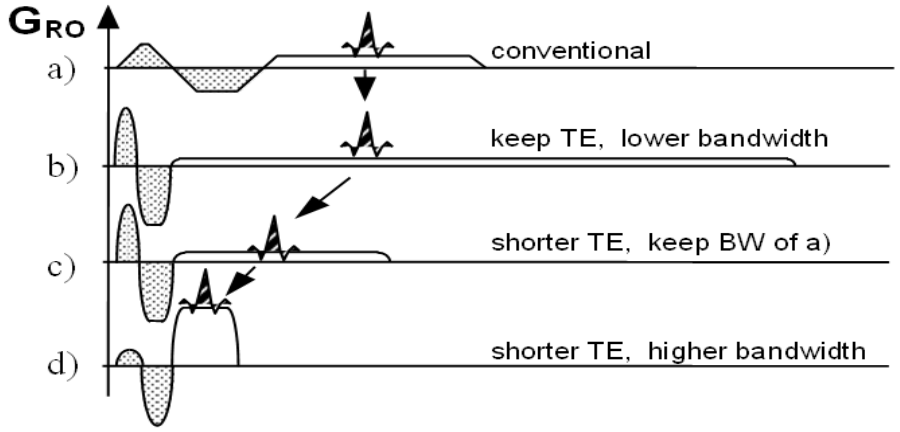

Figure 2: Gradient speed and amplitude improvements and its effect on acquired MR signal.

3 The gradient system

The entire gradient system (Figure 3) is determined by components generating the gradient field, including gradient coil and its driving power devices, i.e., gradient amplifier as well as its connecting elements such as cables and gradient wall filters. The surrounding RF structure of the whole-body, head, and surface RF coils must also be considered in that sense. Eddy currents in this structure may affect the quality of the gradient field.

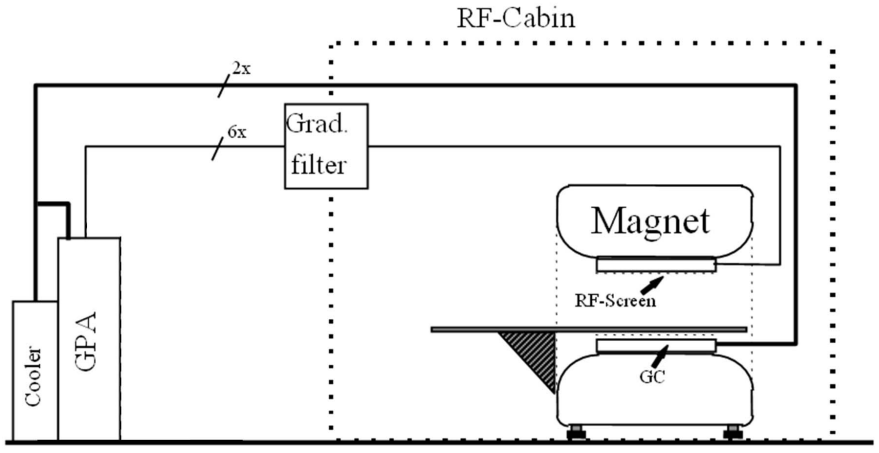

Figure 3: The MR gradient system

3.1 Gradient power loss and cooling

Fast MRI gradients are operated at high currents and voltages thus causing power losses in cables, filters, coil and amplifier; therefore cooling is an important issue. The average power required for a gradient pulse sequence can be calculated analytically as shown in equation [1] for a simplified one dimensional case. A similar relation can be derived considering all three gradient axes.

$$\overline{P/TR} = \frac{1}{TR}\int_{TR} I(t)\cdot V_L\,dt + \frac{1}{TR}\int_{\Delta\nu} \tilde{I}^2(\nu)\cdot R(\nu)\,d\nu + P_o \qquad \text{Equation [1]}$$

The gradient current, I(t), its spectral distribution, $\tilde{I}(\nu)$, and the frequency dependent resistance, R(ν) of the gradient coil is required. The first term represents the losses of the gradient amplifier (V_L characterizes a modeled voltage drop across the gradient amplifier caused by the switching semiconductors), the second term represents the power losses of the gradient coil. P_o is the standby power loss of the gradient system. Figure 4 illustrates this process of calculating the total power consumption of the gradient system.

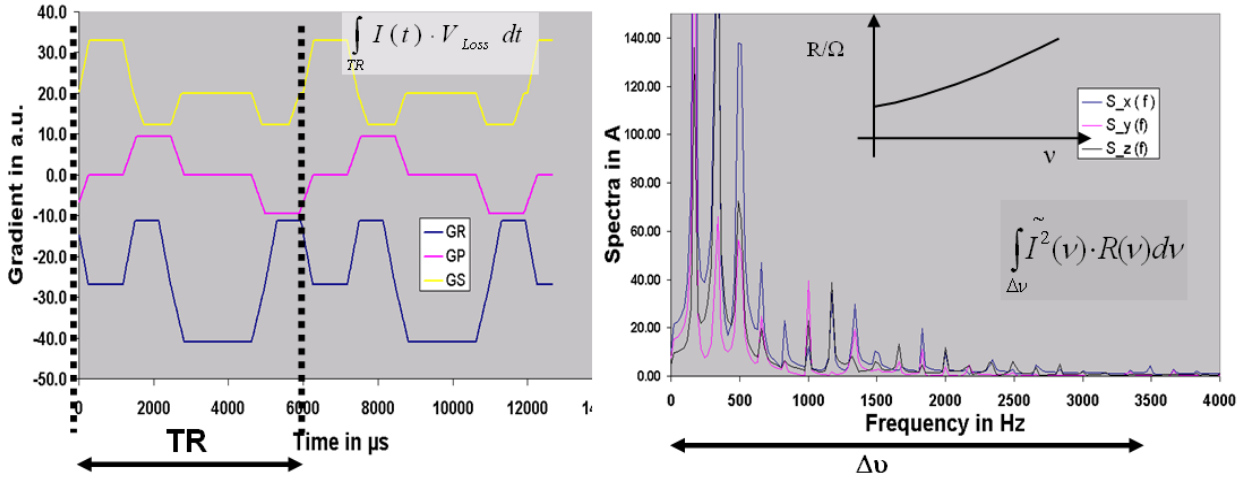

Figure 4: Calculation of gradient power losses. Left) Gradient sequence (TRUE Fisp) timing and its spectra (right) (see text for further explanation)

An alternative, but typically used method to describe the capability of a gradient system in order to withstand the power consumed is described with the so-called gradient power duty cycle (DC), η, otherwise called RMS value, defined as

$$\eta(t_1,t_2) = \frac{\int_{t1}^{t2} G(t)^2\,dt}{G_{\max}^2\,(t_2 - t_1)} \bullet 100\% \qquad \text{Equation [2]}$$

Figure (5) illustrates the process of evaluating the gradient power duty cycle on the example of an EPI sequence. When performing the integration over time, t, and plotting the results (figure 5 right) it can be seen that the DC is high for short integration times and reaches a steady state value usually at times in the order of the repetition time, TR. The values at the steady state DC are commonly referred to as the DC. In this case this sequence requires a DC of 1/50/3% for the PC/RO/SS direction, respectively. It is the obligation of good engineering to design the gradient system in such a manner, that it can withstand the most demanding sequence protocols without forcing it to a safety shut down. Important to note is the fact that the power the gradient system is consuming has to be cooled either by air or by water. For high performance gradient systems water cooling is therefore the first choice allowing the application of fast MRI techniques such as EPI, TurboSE, TrueFisp and related protocols when performed in a continuously running real time imaging mode especially.

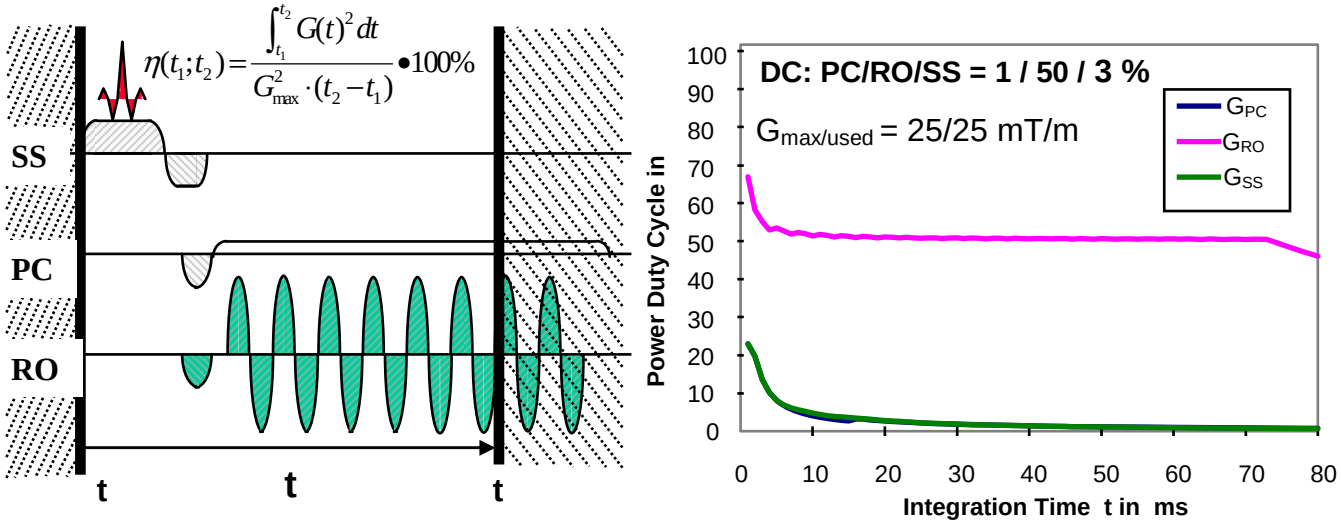

Figure 5: Gradient power duty cycle for an EPI sequence, using sinusoidal gradient pulses. Maximum gradient strength used was 25 mT/m

3.2 Gradient Amplifiers

The purpose of a gradient power amplifier (GPA) is to supply the required voltage, V, and current, I, to the gradient coil of an inductance, L, and a resistance, R, described by

$$V(t) = R \cdot I(t) - L\frac{dI(t)}{dt}$$ Equation [3]

In principle, two different types of gradient power amplifiers can be distinguished. Analogue amplifiers similar to high-precision music amplifiers have been widely spread in the MR market in the early times of MRI. Duty cycles achievable with this type are limited due to losses in the semiconductors. Pulse-width modulated (PWM) amplifiers overcome this drawback and have become the standard for MRI gradient drivers meanwhile.

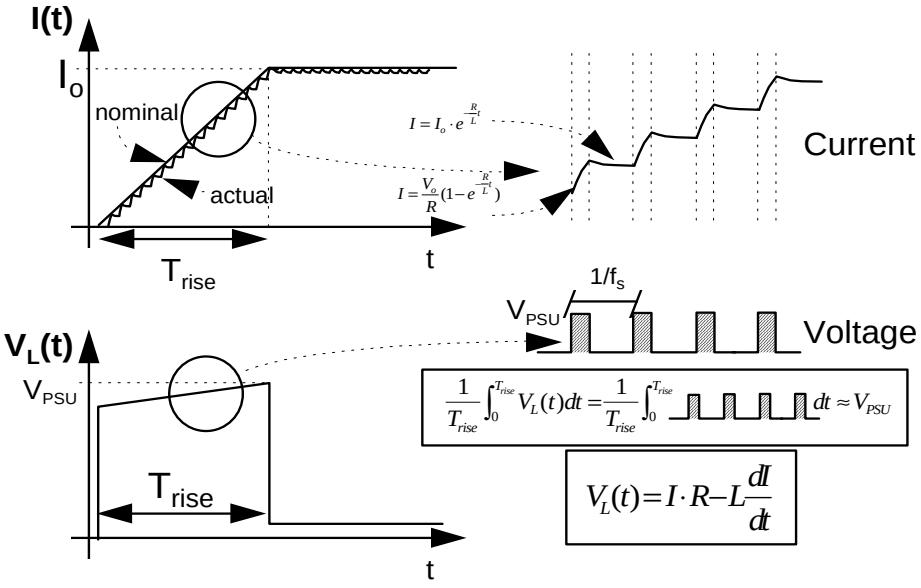

Figure 6: Principle of pulse-width modulated (PWM) amplifiers. Upper row: Gradient current corresponding to a linear ramp (magnified version upper right: In reality those rise and falls are much smoother and ripples can not be seen in the current. They have just been shown here for didactical reasons). Lower row: Voltage required performing the linear ramp and integral condition for the PWM voltage packages.

The basic idea behind PWM amplifiers is that short voltage packages are switched to the coil with frequencies ranging from 20 to 200 kHz or even higher. The voltage required to drive a certain rise time is supplied as described with the integral condition of Figure 6.

Figure 7 shows the principle of modern PWM amplifier. It uses a cascaded version of PWM power stages. In this example, each full bridge provides 400 V and is capable of supplying 500 A. More recent versions even allow higher than 900 A and 2250V. The modulation of these bridges is performed in such a way that an overall output voltage of 2000 V is resulting when required. Figure 8 right shows an oscilloscope snapshot, displaying the current and the unfiltered output voltage of the newly developed amplifier.

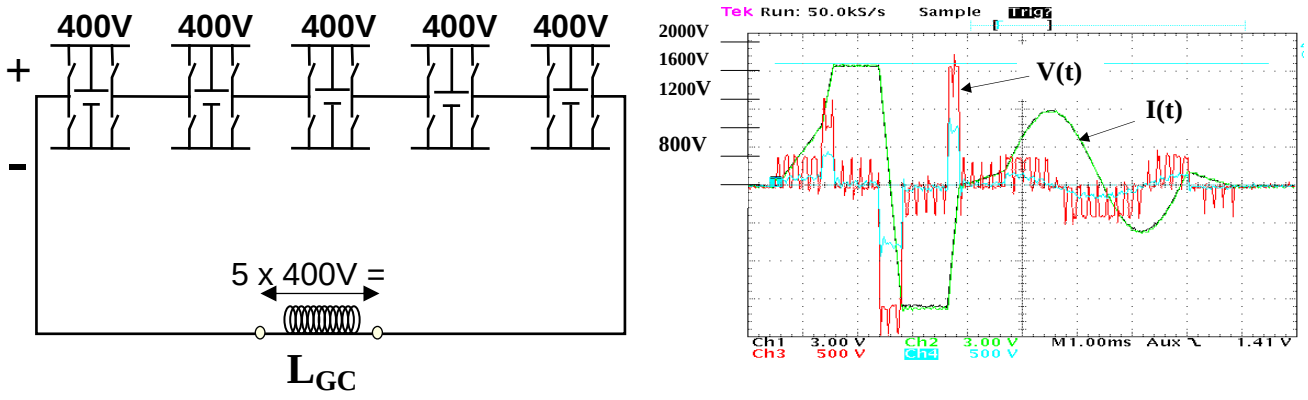

Figure 7: Cascaded PWM amplifier (left) and current and voltage oscilloscope trace (right)

3.3 Gradient Coils

Gradient coil design has most significantly changed over the 1990ties. At the beginning of MRI, only so-called Golay coils[6] were used. First improvements could be achieved as the coil design moved on to polygon design, connecting linear conductors piece by piece, as shown in Figure 8 (left).

Figure 8: Gradient coil winding design of a transverse gradient coil (Y). Left: Polygon design. Right: Finger-print design.

Unshielded designs were common until the introduction of actively screened (AS)[7,8] gradient coils in 1985. These coils consist of a primary (the inner) and a secondary (the outer) coil (Figure 9 left). They are designed such that the required field quality is achieved inside the patient bore and the magnetic flux is ideally zeroed outside the gradient coil at the location of the cryostat (for cylindrical super-conductive magnet systems). That prevents the generation of eddy currents in the cryostat which is essential for high image quality in fast MRI.

Higher gradient amplitudes switched at even higher speed were possible by optimizing the inductance of the gradient coils. This finally led to so-called finger-print coils for x and y gradients, which are now state of the art (Figure 8 right). MRI scanners for the upper market segment now allow amplitudes of 40 - 80 mT/m switched with Slew rates, SR, of 200 T/m/s for EPI applications in a whole-body setting.

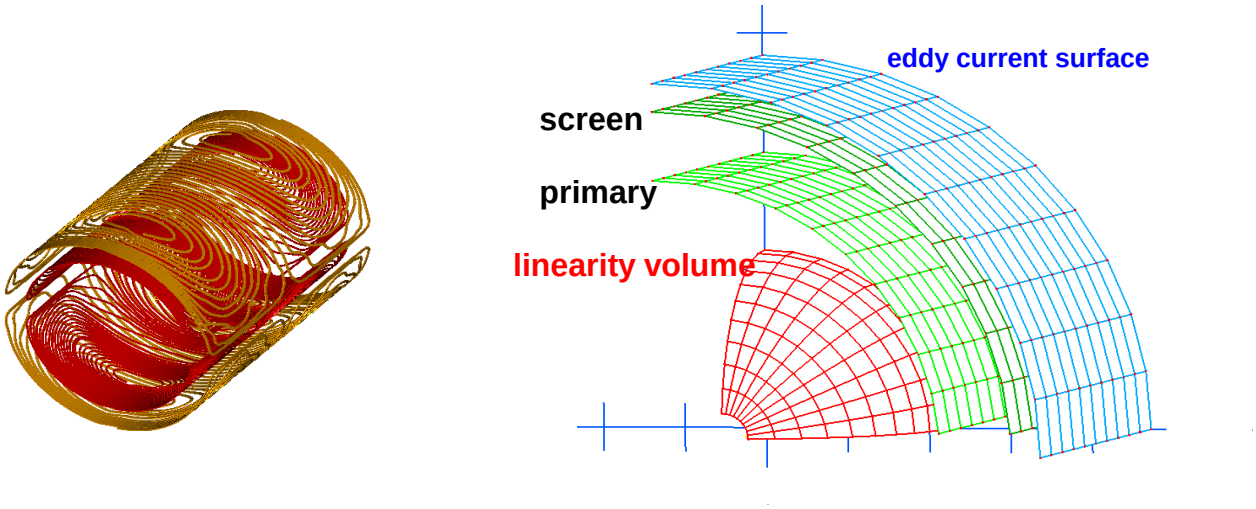

Figure 9: Left) Actively screened (AS) gradient coil (a Y gradient coil is shown). Right) Design optimization. The current distribution in the primary and screen surface is calculated such that the required field quality is reached in the linearity volume, and the flux is minimized at the eddy current surface.

Special purpose applications, such as head-only imaging allow the use of dedicated gradient coils matched to the size of the object to be imaged. Head-gradient coils, used for fMRI and diffusion research applications[9,23] in humans and animals performing at amplitudes of 80 mT/m and above, with slew rates of 400 T/m/s. In the example shown in figure 10, the coil is placed on a crate and can be wheeled in and out of the magnet in a matter of a minute. Switching means are provided to select the whole body gradient coil or the head insert coil. The use for such a coil is optimized for short TE with high b-value diffusion imaging in the head and for monkey imaging with small FOVs.

Figure 10: setup for an easy to exchange head gradient insert allowing higher performance

Cardiac applications require fast and strong gradients. In order to overcome the physiological limits (see chapter 4 and figure 11) accompanying fast gradient switching, a common way so far was to reduce the linearity volume of the gradient coil. In such cases, maximum gradient of 40 mT/m at a rise time of as fast as 200µs (i.e. SR 200) are feasible without causing peripheral nerve stimulation.

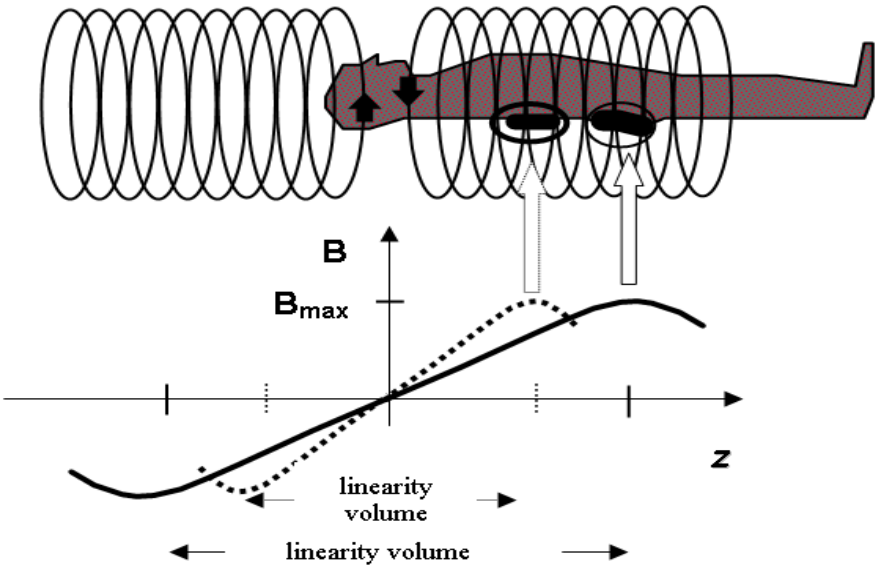

Figure 11: Relation of gradient linearity volume and peripheral nerve stimulation. When shortening the linearity volume, for example of a z gradient coil, the gradient amplitude (the slope of the field plot) can be increased significantly until reaching the same maximum magnetic flux, B_{max}, as possible with the longer gradient coil. This is possible because the maximum exposed magnetic flux defines the stimulation limits (see chapter 4). That principle holds for x and y gradients as well.

The major demand on the design of gradient coils however, comes from the request to shorten the overall length with the widest patient bore of the magnet system in order to reduce the overall cost of MRI systems. Special considerations must be given to power loss[20]. Remember, the power loss dissipates into heat and must therefore be cooled in order to avoid system overheating. Therefore the major goal in gradient design is to minimize power losses. A method to achieve this is shown in figure 12. When shrinking the length of a saddle shaped coil (used for x and y gradients) and keeping the linearity volume constant as shown in figure 12, left, the return paths will get squeezed as close as possible. That in fact has significant effect on the power required to drive the coil as shown with the right graph of figure 12. The power loss is increasing asymptotically when shortening the coil.

In order to minimize the power consumption, the return paths are cut and primary and secondary coil have multiple connections between them. This type of gradient coil design is called three dimensional (3D) coil design. It is different to conventional coils, having typically one connection per coil set only (see figure 12 right). When comparing 3D with conventional gradient coils power consumption is therefore considerably reduced (see figure 12 right). That enables to build magnets shorter with wider inner bore without sacrificing the linearity volume and most important allow to run all types of clinical protocols without forcing the MRI scanner into an overheat condition.

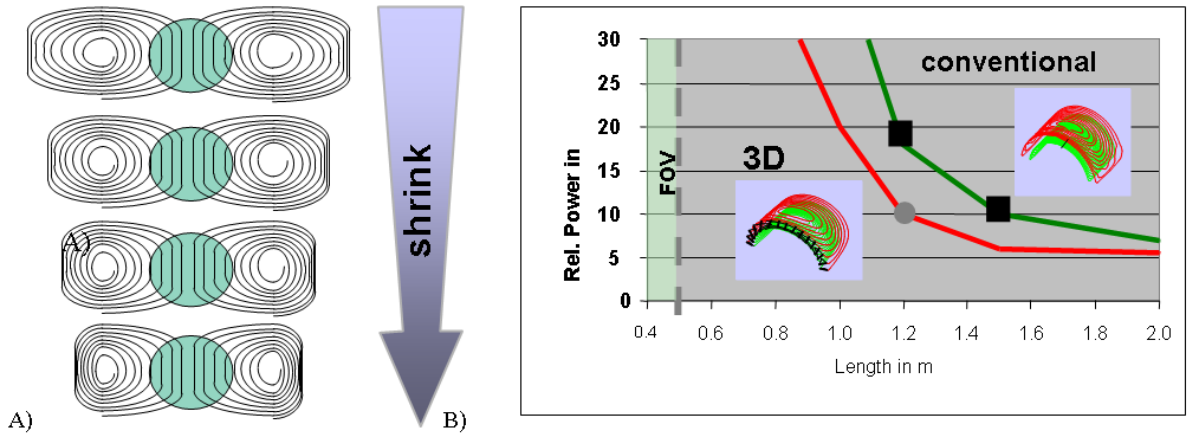

Figure 12: Minimizing the power loss in gradient coils when shrinking gradient coils.

4 Limiting Effects of Fast Gradients

The application of fast and large gradients has some side effects which have its source in the interaction of electro-magnetic fields and forces with the human physiology. On one hand, the very fast switching of gradients can induce electric fields in the human body causing muscle and nerve stimulation. On the other hand, fast and large gradients generate acoustic noise which needs to be taken care of to avoid patient discomfort due to noise.

4.1 Peripheral Stimulation

According to Faraday's law of induction and Maxwell's laws, a time varying magnetic flux, dB/dt, produces an electric field, E, in a conductive environment. For the simple case of a conductive loop of radius, r, penetrated by the flux change dB/dt the induced E field is calculated as

$$E(r) = -c \cdot \frac{r}{2} \cdot \frac{dB}{dt} \qquad \text{Equation [4]}$$

Experimental and theoretical evaluations [11,12,13] have shown that there is a linear relation between the applied magnet flux, B, and the duration of the stimulus, τ, described by the following formula

$$B(\tau) \geq \frac{E_{rheo} \cdot \tau_{chron}}{c \cdot r} \left(1 + \frac{\tau}{\tau_{chron}}\right) \qquad \text{Equation [5]}$$

where c is a geometric factor representing the shape of the exposed body and E_{rheo} and τ_{chron} describe physiological parameters[14,15]. The stimulus duration, τ, is twice the rise time, T_{Rise}, of the gradient pulse in our case.

Figure 13 illustrates results obtained from two different gradient pulse trains (trapezoidal and sinusoidal). A linear relation can be found theoretically, as expressed with equation [5], and has been proved experimentally as well[13]. When considering the dependency of thresholds expressed as function of gradient pulses, an asymptotic relation can be found that illustrates that after typically 16 pulses the minimum of the threshold is reached.

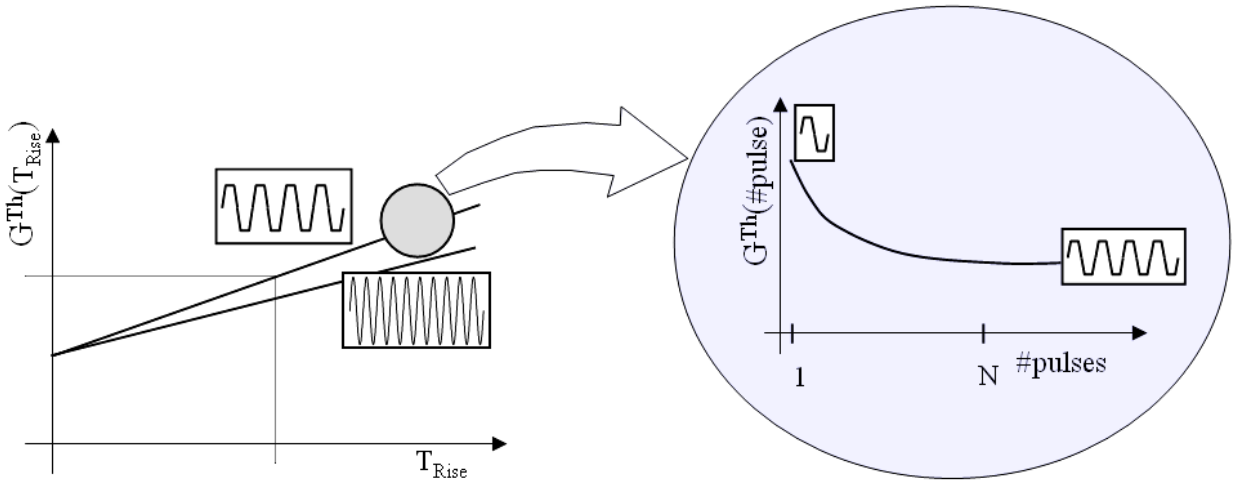

Figure 13: Illustration of the threshold gradient strength as a function of the gradient pulse rise time (left) and the number of applied pulses.

4.2 Acoustic Noise

With the introduction of fast MRI techniques the acoustic noise became more and more relevant because it can reach noise levels which can cause discomfort or harm to patients and personnel. Therefore limits for maximum acoustic noise set by regulatory bodies[16,17] have to be applied to MRI. The acoustic noise is caused by the so-called Lorentz force.

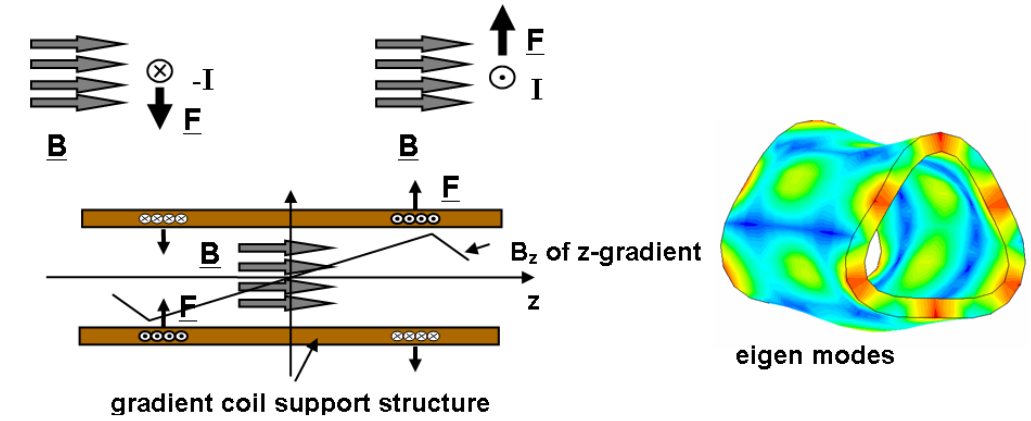

Figure 14: Upper left: Lorentz forces on a wire carrying current, I, exposed to a magnetic flux, B: Force F pointing upward when the current flows towards the observer. When the current is directed away (indicated by -I) from the observer the force points downward. Lower left: For a z-gradient coil both cases are simultaneously present. A positive current (generating an elevation of the flux at positive z positions) expands the coil structure on the right side and contracted it on the left side. When the current polarity is changed, the contraction and expansion is altered, respectively. That causes compression and depression of the air inside the gradient bore and produces acoustic noise. Right: complex oscillating pattern are created which are called eigen modes

When a current passing through a wire is exposed by a magnetic flux (figure 14) a force perpendicular to the current and the magnetic flux is generated. Mathematically this is expressed by the vector product (*x*)

$$\underline{F} \sim \underline{I} \times \underline{B} \qquad \text{Equation [6]}$$

where F is the force acting on the wire, I is the electric current through the wire and B is the magnetic flux exposing the wire. All quantities are described as vectors.

In MR scanners, the main magnetic flux, B, and the current through the gradient coils generate a deformation of the coil structure. This effect causes vibrations similar to a loud speaker and therefore produces acoustic noise. The amplitude of the acoustic noise is largest when a maximum current in combination with a minimum rise time, is pulsed through the coil. The highest noise level that can be generated will occur when all three gradient axes are pulsed at the same time. In general, gradient coils have several modes of oscillations, the so-called eigen modes[18,19,20] depending on their geometrical dimensions and material properties such as weight and stiffness. Lorentz forces are proportional to the magnet field of the MRI scanner as indicated by Equation 6. Clinical scanner now come from .2 up to 3 Tesla, while human research scanner now reach ultra high field (UHF) strength of 7 Tesla and 9.4 Tesla, posing a tremendous challenge on the gradient coil structure due to the Lorentz forces.

4.3 Eddy Current Effects

Modern style gradient coils are fully screened in order to avoid eddy current effects in the MR image. The design of a screened gradient coil is done such that the effect of the eddy currents in the volume of interest (VOI), i.e. the patient scanning region, is ideally zeroed. However, residual eddy currents are always present due to technical limitations. Eddy currents are induced in metallic structures inside and surrounding the gradient coil. Outside the gradient coil the most dominant source of eddy current is the cryo shield. Inside the gradient coil RF coils as well as the RF screens (see figure 15) are fully exposed to the gradient fields.
Eddy currents in the RF screen can create heat inside the patient bore and therefore pose an additional heat source besides RF Power deposition. Therefore gradient eddy current paths have to be interrupted as far as possible. This is achieved by slotting the RF structures[10] and bridging the gaps with capacitors allowing to pass RF currents and preventing gradient eddy currents. The issue of gradient eddy currents holds for all RF coils (body, head and surface coils).

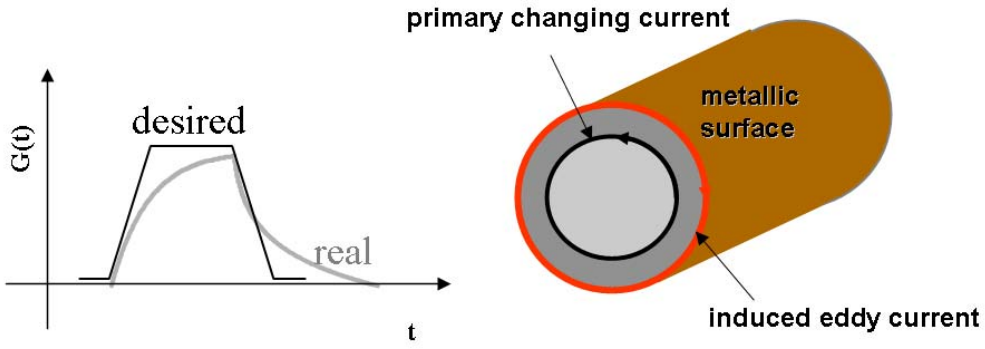

Figure 15: Eddy currents: Filtering effects on gradient pulses

Eddy currents have a filtering effect on the applied gradient pulses (figure 15 left) and are a major cause for imaging artifact. EPI in particular is vulnerable to severe so-called N/2 -ghosting as shown in Figure 16. Very short eddy current time constants in the order of the rise time, T_{Rise}, (created in the RF structure) are responsible for this type of artifact. Eddy current time constants on the order of the duration from one RF pulse to the other cause shading artifacts in TSE or TGSE imaging. Artifacts of this kind are segmentation dependant as well. Finally, long term eddy currents can cause frequency drifts due to the eddy current tails after a gradient pulse causing problems when fat saturation is applied. Insufficient fat or water suppression can therefore result.

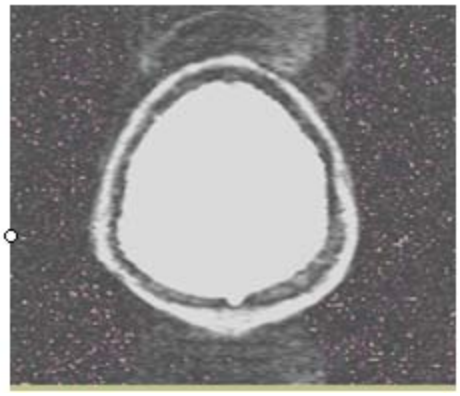

Figure 16: Eddy currents and its effect on image quality.

4.4 Eddy current compensation

Although residual eddy currents are usually very small, applying eddy current compensation, ECC, is mandatory. This is performed by pulsing a trapezoidal gradient pulse and detecting the magnetic field "tail" $B_{EC}(t)$ after the gradient pulse is switched off. Below I explain the first case, i.e long decay times.

In the old days of MRI this was performed by using magnetic field pick up coils (see Figure 17). The induced voltage in that coil was detected, while pulsing a trapezoidal gradient pulse. The induced voltage, V_{ind}, is proportional to the flux change $dB_{EC}(t)/dt$. In order to achieve $B_{EC}(t)$ an integration step had to be introduced. This was achieved by an electronic circuit which integrated the induced voltage over time, yielding the desired $B_{EC}(t)$. Two symmetric positions, +/- z_o, of the field probe are required to calculate the eddy current per gradient axis, respectively.

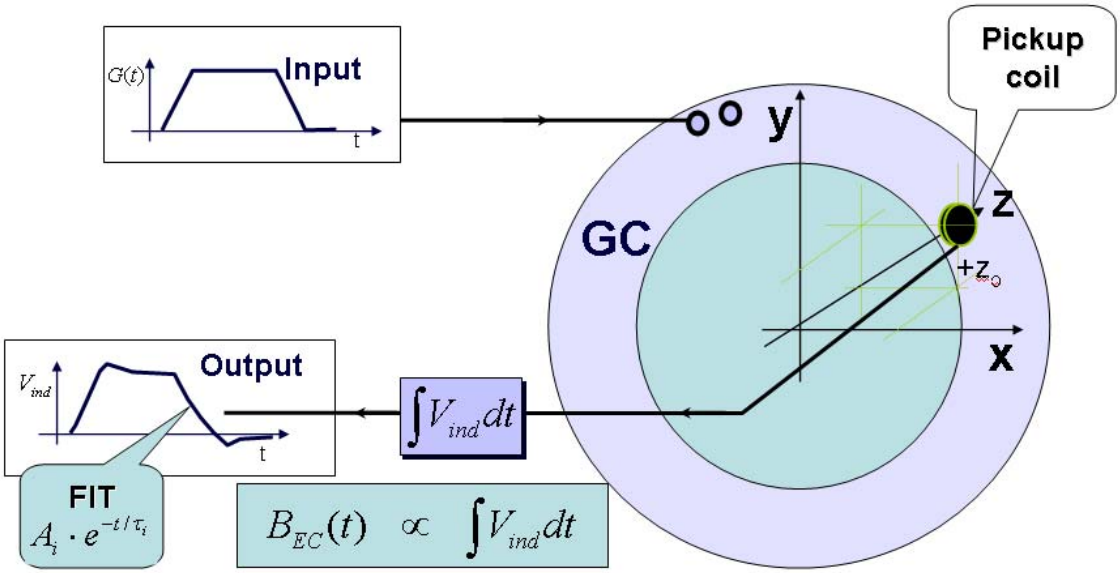

Figure 17: Eddy current measurement with pick up probes

This pickup coil technique was very susceptible to integrator drift and was discarded later on because better techniques have been developed. Modern MRI scanner now use an MRI experiment to detect these eddy current induced $B_{EC}(t)$. This is illustrated in Figure 18. In this case a gradient pulse is pulsed prior to a spin echo (SE) experiment. The excitation pulses are slice selective and excite a slice of about $5mm^3$ at symmetric positions +/- z_o for a z-gradient. Analogous +/- x_o and +/-y_o excitation is used for x and y-gradients, respectively. The phase $\Phi(t)$of the Spin Echo (SE) signal is then differentiated yielding the eddy current magnetic flux $B_{EC}(t) = d\Phi(t)/dt$. The delay time τ is

incremented to accommodate the different eddy current time constants. In general the eddy current generated flux at a point located at z_o is described by $B_{EC}(z_o) = B_o + G_z \cdot z_o$. The calculated $B_{EC}(t)$ of a z-gradient can therefore be composed as $B_{EC}(t) = B_o(t) + B_{Gz}(t)$. Thus one has to compensate a gradient like eddy current, B_{Gz}, and a B_o like eddy current as illustrated in the upper right section of Figure 18. The fitted amplitude A_i and time constants τ_i are then used for compensating the eddy currents. In modern MRI scanners this is performed digitally. A_i and τ_i are used as input to a digital filter to pre-distort the gradient pulses appropriately so that in the end a perfect trapezoidal gradient pulse is resulting.

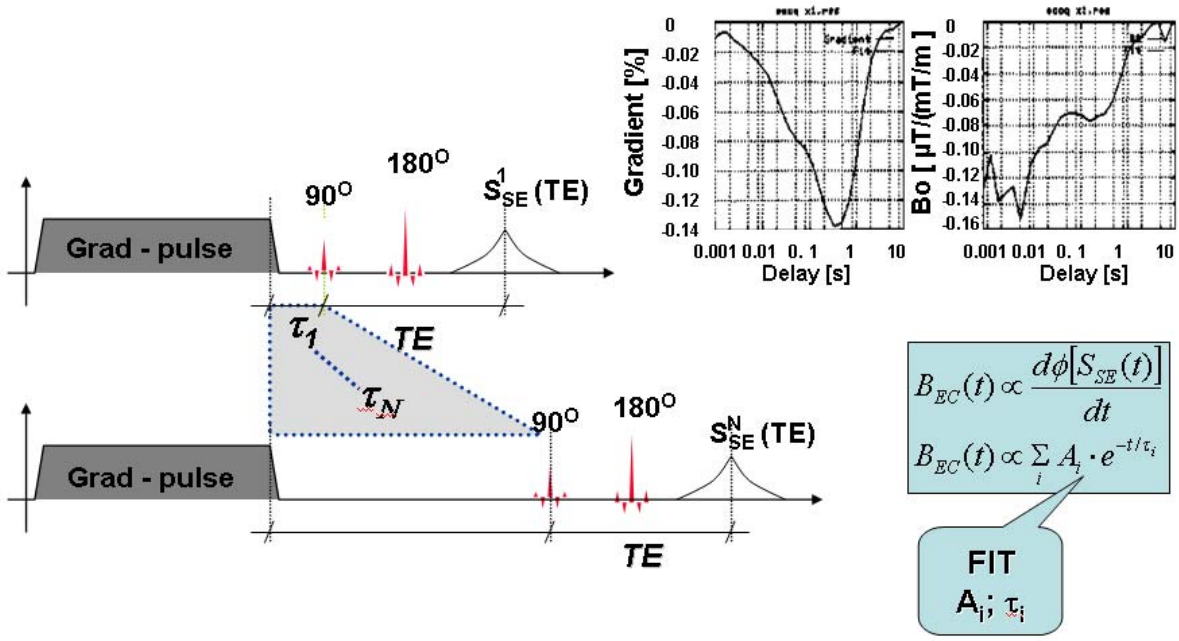

Figure 18: Eddy current measurement with MRI

5 Conclusion

The improvements on gradient hardware was the driving force for the development of fast MRI. MRI techniques, such as EPI TrueFISP and short TE applications for MR angiography, benefit most from these developments. From a technical point of view, further progress is still possible when using parallel imaging techniques such as SENSE[22] and GRAPPA[23]. When combined, high performance gradients and parallel imaging techniques, even faster imaging techniques can evolve which allow a reduction in SAR burden. However, adverse effects on the human physiology caused by acoustic noise and peripheral stimulation seem to mark an end for future improvements. Unless these side effects are not eliminated or at least significantly minimized, no real performance increase of gradients can be expected.

6 References

1 Mills C, Lukes S, Norman D, Newton TH, Brant-Zawadzki M, Crooks L, Sheldon P and Kaufman L. Normal and Abnormal Anatomy of the head: dependency on imaging techniques and parameters. SMRM Book of abstracts 1982, Boston MA, pg107

2 Mansfield P. Multi-planar image formation using NMR spin echoes. J. Phys. C. 1977; 10: L55-L58.

3 Schmitt F, Stehling MK, Ladebeck R, Fang M, Quaiyumi A, Bärschneider E, Huk W. Echo-planar imaging of the central nervous system at 1.0 T. JMRI 1992; 2: 473-478.

4 Mueller OM., Roemer P., Park JN. and Souza SP. A general purpose non-resonant gradient power system. Proceedings of the 10th Annual Scientific Meeting of the SMRM, 1991, San Francisco, p. 130.

5 Ideler KH, Nowak S, Borth G, Hagen U, Hausmann R and Schmitt F. A resonant multi purpose gradient power switch for high performance imaging. Proceedings of the 11th Annual Scientific Meeting of the SMRM, 1992, Berlin, p. 4044.

6 Golay MJE, Magnetic field control apparatus. 1957: US Patent 3,515,979.

7 Roemer P., Edelstein W.A. and Hickey J. Self shielded gradient coils. Proceedings of the 5th Annual Meeting of the SMRM, 1986, Montreal, p 1067.

8 Mansfield P, Chapman B, Turner R and Bowley R. Magnetic field screens. 1985: UK Patent 2 180 943 B, US Patent 4978920.

9 Ogawa S, Lee T-M Kay AR, Tank DW. Brain magnetic resonance imaging with contrast dependent on blood oxygenation. Proc Natl Acad Sci USA (1990),87:9868-9872

10 Renz W, Dürr W and Oppelt R. A reduced size body resonator for fast imaging techniques. Proceedings of the 2nd Annual ScientificMeeting of the SMR, 1994, San Francisco, p. 1113.

11 Budinger TF, Fischer H, Hentschel D, Reinfelder H-E and Schmitt F. Physiological effects of fast oscillating magnetic flux gradients. J Comp Ass Tomog 1991; 15: 909-914

12 F. Schmitt, P. Wielopolski, H. Fischer, R.R. Edelman. Peripheral Stimulation and their Relation to Gradient Pulse. Proceedings of the Society of Magnetic Resonance, 1994, pg 102

13 Irnich W. Magnetostimulation in MRI. Proceedings of the Society of Magnetic Resonance, 1993, pg 1371

14 Irnich W (1980) The chronaxie time and its practical importance. PACE 3: 292-301

15 Recoskie, B.J., Scholl, T.J., Chronik, B.A. (2009). The discrepancy between human peripheral nerve chronaxie times as measured using magnetic and electric field stimuli: the relevance to MRI gradient coil safety. *Physics in Medicine and Biology*, 54, 5965-79.

16 NEMA Standards Publication No. MS 4-1989: Acoustical Noise Measurement Procedure for Diagnostic Magnetic Resonance Imaging devices. National Electrical Manufacturers Association 2101 L Street, N.W. Washington, D.C. 20037

17 European Standard pr EN 60601-2-33; 1995.

18 Haiying L, Junxiao L. Gradient coil mechanical vibration and image quality degradation. Proceedings of the Society of Magnetic Resonance, 1996, pg 1393

19 Hedeen RA, Edelstein W. Characterization and prediction of gradient acoustic noise in MR imagers. Proceedings of the Society of Magnetic Resonance, 1996, pg 1389

20 Sellers M. A new method of quantifying the acoustic noise of MRI devices. Proceedings of the Society of Magnetic Resonance, 1996, pg 1390

21 Schmitt F., Arz W., Eberlein E., et al. An ultra-high performance gradient system for cardiac and neuro MR Imaging. Proceedings of the ISMRM, 199, p470.

22 K. P. Pruessmann, M. Weiger, M. B. Scheidegger, P. Boesiger, SENSE: Sensitivity encoding for fast MRI, MRM 42:952-962 (1999)

23 Griswold MA, Jakob PM, Heidemann RM, et al. Generalized autocalibrating partially parallel acquisitions (GRAPPA). *Magn Reson Med*. 2002;47:1202–1210.